Fundamental and vortex solitons in a two-dimensional optical lattice

Jianke Yang

Department of Mathematics and Statistics, University of Vermont, Burlington, Vermont 05401

Ziad H. Musslimani

Department of Applied Mathematics, University of Colorado, Campus Box 526, Boulder, Colorado 80309-0526

Received April 11, 2003

Fundamental and vortex solitons in a two-dimensional optically induced waveguide array are reported. In the strong localization regime the fundamental soliton is largely confined to one lattice site, whereas the vortex state comprises four fundamental modes superimposed in a square configuration with a phase structure that is topologically equivalent to the conventional vortex. However, in the weak localization regime, both the fundamental and the vortex solitons spread over many lattice sites. We further show that fundamental and the vortex solitons are stable against small perturbations in the strong localization regime. © 2003 Optical Society of America

OCIS code: 190.0190.

Optical wave propagation in periodic lattices (such as an array of optical waveguides) exhibit many new phenomena that arise solely from the existence of allowed bands and forbidden gaps in the linear spectrum. In these periodic structures, wave dynamics is governed by the interplay between optical tunneling to adjacent sites (or waveguides) and nonlinearity. A balance between these two effects could result in self-localized structures known as lattice solitons.[1]

Lattice solitons in waveguide arrays were first predicted to exist as solutions to the discrete nonlinear Schrödinger equation[2] and later observed in AlGaAs waveguide arrays.[3] This experimental observation stimulated much new research, such as studies of solitons in two-dimensional (2D) photorefractive optical lattices in which localization phenomena have been observed.[4–6]

In this Letter, fundamental and vortex solitons in a 2D optical lattice are reported, and their stability is analyzed. In the strong localization regime, the fundamental soliton is confined largely to one lattice site with a uniform phase. The vortex soliton comprises four fundamental modes located at the bottoms of the optical potential in a square configuration with a phase structure that is topologically equivalent to a conventional vortex. By winding around the zero intensity position along any simple closed curve, the phase of the vortex state acquires a 2π increment. We call this structure a vortex cell. When the localization is weak, both fundamental solitons and vortex cells spread over many lattice sites. In the strong localization regime, we show that the fundamental soliton as well as the vortex cell is stable under weak- perturbations.

We begin with the 2D nonlinear Schrödinger equation

$$i\,\frac{\partial\psi}{\partial z} + \left(\frac{\partial^2}{\partial X^2} + \frac{\partial^2}{\partial Y^2}\right)\psi - V\psi + |\psi|^2\psi = 0\,, \qquad (1)$$

where $V = V_0(\cos^2 X + \cos^2 Y)$ is the optical lattice potential and V_0 is its intensity. We can obtain such a potential by optically interfering two pairs of laser beams.[6] Here, we consider the focusing Kerr nonlinearity, which is different from the saturable nonlinearity in recent experiments with 2D photorefractive lattice solitons.[4–6] However, our results can be readily extended to the saturable case and directly applied to the Bose–Einstein condensation in 2D optical lattices. If the potential parameter $V_0 < 0$, one can use a transformation $X \to X + \pi/2$, $Y \to Y + \pi/2$, and $\psi \to \psi \exp(-2iV_0 z)$ to convert it to the $V_0 > 0$ case. Thus we assume that $V_0 > 0$ in this Letter without any loss of generality. Without the lattice potential, solitons would collapse under small perturbations.[7] However, as we show here, optical lattices can suppress the collapse of fundamental solitons and vortex cells. Equation (1) conserves two quantities; the power, $P = \int_{-\infty}^{\infty}\int_{-\infty}^{\infty}|\psi|^2\,dX\,dY$, and the energy, E:

$$E = \int_{-\infty}^{\infty}\int_{-\infty}^{\infty}\left\{|\nabla\psi|^2 - \frac{1}{2}\,|\psi|^4 + V|\psi|^2\right\}dX\,dY\,. \qquad (2)$$

We look for stationary solutions of the form $\psi(X,Y,z) = \exp(-i\mu z)u(X,Y)$, where μ is the propagation constant of the soliton. Then $u(X,Y)$ satisfies

$$\frac{\partial^2 u}{\partial X^2} + \frac{\partial^2 u}{\partial Y^2} - Vu + |u|^2 u = -\mu u\,. \qquad (3)$$

A fundamental soliton of Eq. (3) has a single main hump sitting at the bottom of the potential, say, $(X,Y) = (\pi/2, \pi/2)$. Two examples corresponding to propagation constants $\mu = 0$ and 0.88 with $V_0 = 1$ are displayed in Figs. 1(c) and 1(d). One can see that for small μ [Fig. 1(c)], the beam is largely confined to one lattice site, whereas at higher μ [Fig. 1(d)], it spreads over many lattice sites. Similar solutions in different physical contexts (photonic crystals and Bose–Einstein condensation) are known to exist, too,[8–10] even though the mathematical models or physics are quite different. To quantify these fundamental solitons, we calculate the dependence of normalized power P on propagation constant μ for $V_0 = 1$, as displayed in Fig. 1(a). When $\mu \to -\infty$, P approaches a constant 11.70. This is apparently

0146-9592/03/212094-03$15.00/0

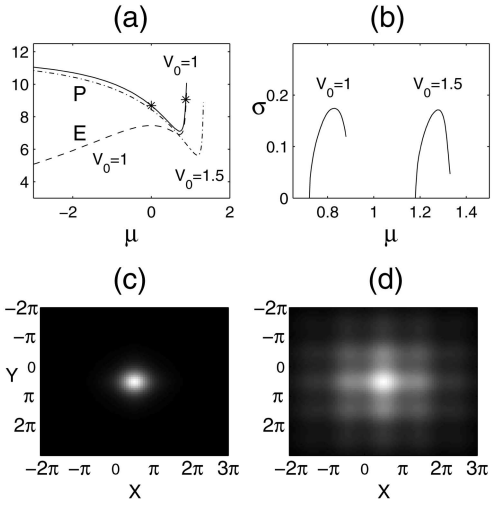

Fig. 1. (a) Normalized power P (for $V_0 = 1$, 1.5) and energy E (for $V_0 = 1$) of fundamental solitons versus μ. (b) Unstable eigenvalues σ of these solitons. (c) and (d) Profiles of fundamental solitons at $\mu = 0$ and $\mu = 0.88$ ($V_0 = 1$), respectively.

because in this limit the fundamental soliton is highly localized; thus it approaches the lattice-free fundamental-soliton state, which has critical power $P_c \approx 11.70$. As μ reaches a cutoff value of approximately 0.95, P appears to go to infinity. In this limit the fundamental state becomes uniformly distributed in space. Thus, this cutoff value should be the boundary of the bandgap in the linear-wave spectrum. When $\mu \approx 0.72$, $dP/d\mu$ changes sign. The Vakhitov–Kolokolov (VK) theorem suggests that at this μ value the stability of these solitons must change.[11] We have confirmed this prediction by numerically simulating the linearized version of Eq. (1) around the soliton described above. When $\mu > 0.72$, a purely real unstable eigenvalue indeed exists and is shown in Fig. 1(b). When $\mu < 0.72$, unstable eigenvalues do not exist, and hence these solitons are linearly stable.

For the 2D self-focusing case, collapse is an important issue. The linear stability analysis described above does not guarantee that the fundamental soliton will not collapse under small perturbations. In the study of collapse the energy, E, plays an important role. In the absence of the lattice potential or when the potential is harmonic,[12] the soliton collapses if its energy is negative. In case the energy is positive, however, the soliton collapses only if it is strongly perturbed. For the optical lattice, we have calculated the energy, E, of fundamental solitons at various values of μ and plotted the results in Fig. 1(a). The energy is found to be always positive. Thus we can expect that this state is able to withstand small perturbations without collapse. To confirm this expectation, we numerically study the nonlinear evolution of the fundamental soliton under small perturbations by directly simulating Eq. (1) with initial condition

$$\psi(X, Y, z = 0) = u(X, Y)[1 + \varepsilon u_p(X, Y)], \qquad (4)$$

where $\varepsilon \ll 1$, and $u_p(X, Y)$ is the initial perturbation. We first take u_p to be white noise. A large number of simulations with small ε and various realizations of random-noise perturbations have been performed, and we have found that for $V_0 = 1$, if $\mu < 0.72$, the fundamental soliton is indeed stable against white-noise perturbations; when $\mu > 0.72$, the soliton is unstable. To study the nonlinear evolution process, we now take $u_p = 1$. For $V_0 = 1$, $\mu = 0$, and $\varepsilon = \pm 0.01$, nonlinear evolutions are plotted in Fig. 2(a). We see that the perturbed soliton oscillates only weakly around the fundamental-soliton state, meaning that the soliton is both linearly and nonlinearly stable. On the other hand, at $V_0 = 1$ and $\mu = 0.88$ (where the soliton is linearly unstable), the dynamics is different, as two situations are identified: (i) at higher input power ($\varepsilon > 0$) the perturbed state relaxes into a z-periodic bound state [Figs. 2(b) and 2(c)], and (ii) at lower input power ($\varepsilon < 0$) the perturbed state decays into linear Bloch waves [Figs. 2(b) and 2(d)]. Similar situations can be found in Ref. 13 for a different system.

In addition to the fundamental solitons, we have numerically found vortex solitons. Two examples with $V_0 = 1$, $\mu = 0$, and 0.82 are shown in Figs. 3(b)–3(d). At $\mu = 0$ (strong localization regime), the vortex state comprises four fundamental solitons superimposed in a square configuration with a phase structure that is topologically equivalent to a conventional vortex [see Figs. 3(b) and 3(c)]. By winding around the center along any closed curve, the phase of the vortex acquires a 2π increment and thus we name it a vortex cell. At $\mu = 0.82$ (weak localization regime), the vortex cell spreads out to more lattice sites and becomes more intricate, as can be seen from Fig. 3(d). But its phase structure is almost the same as with $\mu = 0$. We should point out that these vortex cells are different from conventional vortices without an optical lattice in a major aspect: The vortex cells' intensities and phase depend on both r and θ. These vortex cells (especially in the strong localization regime) might be related to the lattice vortices reported in Ref. 14. Normalized power and

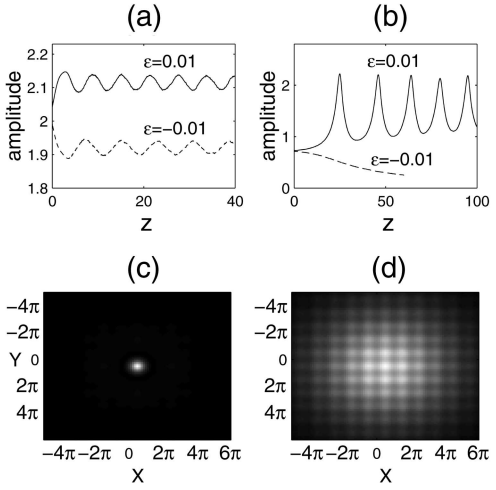

Fig. 2. Nonlinear evolution of fundamental solitons under perturbations [Eq. (4)] for (a) $V_0 = 1$, $\varepsilon = \pm 0.01$, $u_p = 1$, and $\mu = 0$ and (b) $\mu = 0.88$. Snapshots of the soliton intensity corresponding to the dynamics depicted in (b) for (c) $\varepsilon = 0.01$, $z = 80$ and (d) $\varepsilon = -0.01$, $z = 60$.

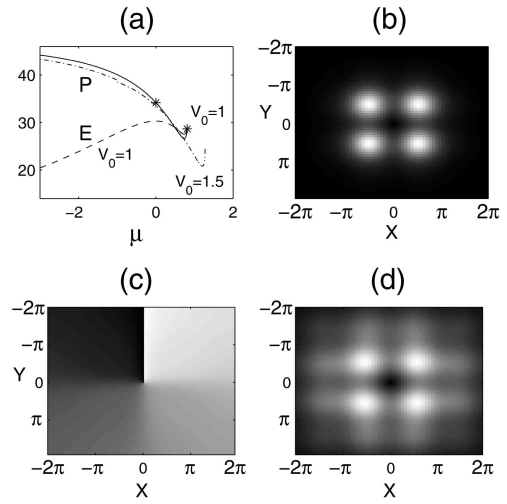

Fig. 3. (a) Normalized power P (for $V_0 = 1$, 1.5) and energy E (for $V_0 = 1$) of vortex cells versus μ. (b), (d) Intensity plots of vortex cells with $V_0 = 1$, $\mu = 0$ and $\mu = 0.82$, respectively. (c) Phase plot of the vortex cell in (b).

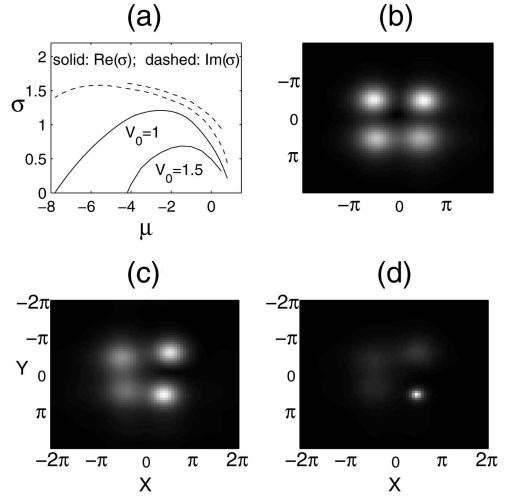

Fig. 4. (a) Unstable eigenvalues of vortex cells for $V_0 = 1$. (b)–(d) Instability development of the vortex with $V_0 = 1$ and $\mu = 0$ [see Figs. 3(b) and 3(c)] when it is initially amplified by 1%; intensity plots at z values of 50, 51.5, and 52 are shown in (b), (c), and (d), respectively.

energy diagrams versus the propagation constant of these vortex cells at $V_0 = 1$ are shown in Fig. 3(a). Unstable eigenvalues σ of vortex cells are determined by simulation of linearized equation (1) around vortex cells. The results are shown in Fig. 4(a) for $V_0 = 1$. One can see that the vortex cells experience oscillatory instability at $\mu > -7.8$ and become stable at $\mu < -7.8$. These vortex cells also suffer VK instability in the region $\mu > 0.73$, where $dP/d\mu > 0$ [see Fig. 3(a)]. However, the oscillatory instability is much stronger, as it occurs over a wider region and has a higher growth rate.

Figure 3(a) shows that vortex cells also have positive energy. Thus, if a vortex cell is linearly stable, it should be able to resist collapse under small perturbations.[12] However, if the vortex cell suffers the linear oscillatory instability discussed above, this instability could result in power exchange from one part of the cell to another so that the intensity at some small spots becomes high, triggering local collapse. We have observed this situation numerically. An example is shown in Figs. 4(b)–4(d), which display the development of a vortex cell with $\mu = 0$ and $V_0 = 1$ when it is amplified by 1% initially.

We next discuss the effect of varying potential strength V_0 on the formation and stability of fundamental and vortex solitons. For this purpose, we have chosen $V_0 = 1.5$ and repeated most of the calculations presented above. The results are displayed in Figs. 1(a), 1(b), 3(a), and 4(a). One can see that (i) at higher potential, both the fundamental and the vortex solitons exist at wider ranges of μ values, and their minimal powers decrease; and (ii) the VK instability of fundamental solitons remains similar, but the oscillatory instability of vortex cells is strongly reduced. Thus we conclude that higher lattice potential stabilizes vortex cells.

In conclusion, we have studied new types of fundamental and vortex solitons in a 2D optical lattice potential and shown that both solitons are stable in the strong localization regime.

J. Yang's e-mail address is jyang@emba.uvm.edu.

References

1. F. Lederer and Y. Silberberg, Opt. Photon. News **13**(2), 48 (2002).
2. D. N. Christodoulides and R. J. Joseph, Opt. Lett. **13,** 794 (1988).
3. H. Eisenberg, Y. Silberberg, R. Morandotti, A. Boyd, and J. Aitchison, Phys. Rev. Lett. **81,** 3383 (1998).
4. N. Efremidis, S. Sears, D. N. Christodoulides, J. Fleischer, and M. Segev, Phys. Rev. E **66,** 046602 (2002).
5. J. Fleischer, T. Carmon, M. Segev, N. Efremidis, and D. N. Christodoulides, Phys. Rev. Lett. **90,** 023902 (2003).
6. J. Fleischer, M. Segev, N. Efremidis, and D. N. Christodoulides, Nature **422,** 147 (2003).
7. P. L. Kelley, Phys. Rev. Lett. **15,** 1005 (1965).
8. P. Xie, Z. Zhang, and Z. Zhang, Phys. Rev. E. **67,** 026607 (2003).
9. A. Ferrando, M. Zacares, P. Cordoba, D. Binosi, and J. A. Monsoriu, Opt. Express **11,** 452 (2003), http://www.opticsexpress.org.
10. B. B. Baizakov, B. A. Malomed, and M. Salerno, Europhys. Lett. **63,** 642 (2003).
11. N. G. Vakhitov and A. A. Kolokolov, Izy. Vyssh. Uchebn. Zaved Radiofiz. **16,** 1020 (1973).
12. L. P. Pitaevskii, Phys. Lett. A **221,** 14 (1996).
13. D. E. Pelinovsky, V. V. Afanasjev, and Yu. S. Kivshar, Phys. Rev. E **53,** 1940 (1996).
14. B. A. Malomed and P. G. Kevrekidis, Phys. Rev. E **64,** 026601 (2001).